

## 1. Introduction

Materials science makes extensive use of **coarse-grained** models for the dynamics and growth of **solid** and **melt** phases. In particular, so called **Phase-Field** models are used for the determination of macroscopic properties. This theory can be derived from a simplification of the **Dynamical Density Functional Theory** [1].

This effective approach implies that **few density modes** are sufficient for the description of the dynamics. We test this assumption on a simple **non-equilibrium** model for crystal growth, comparing **numerical simulations** and **3d DDFT calculations**.

## 2. Langevin dynamics of LJ particles

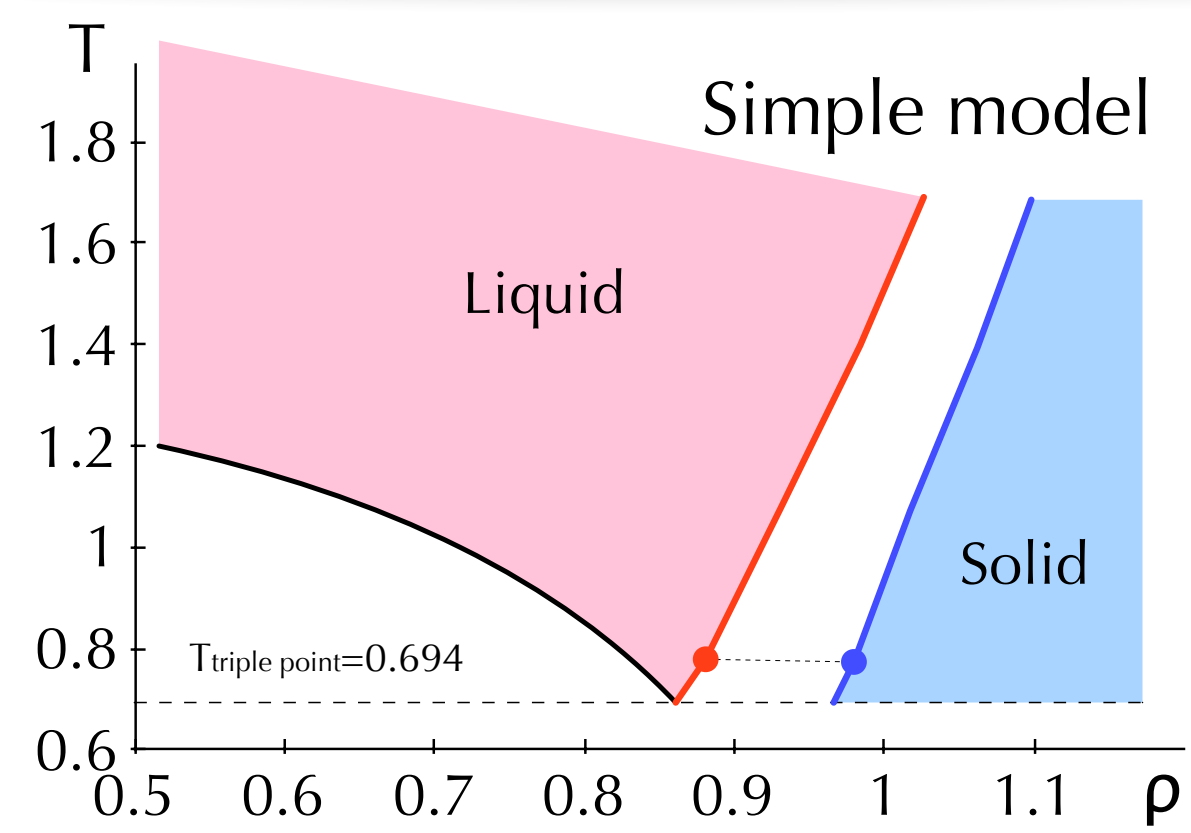


Fig.1 LJ phase diagram: melting line.

**Planar growth** of a crystal of **Lennard-Jones** particles.

- **Langevin dynamics** (for comparison with DDFT where Brownian motion is assumed)
- **NVT ensemble**.
- **Fixed structured perfect fcc walls** exposing the [100] orientation to the liquid.
- **Metastable liquid** such that  $\rho_{liq} = \rho_{sol} = 0.9732$ .

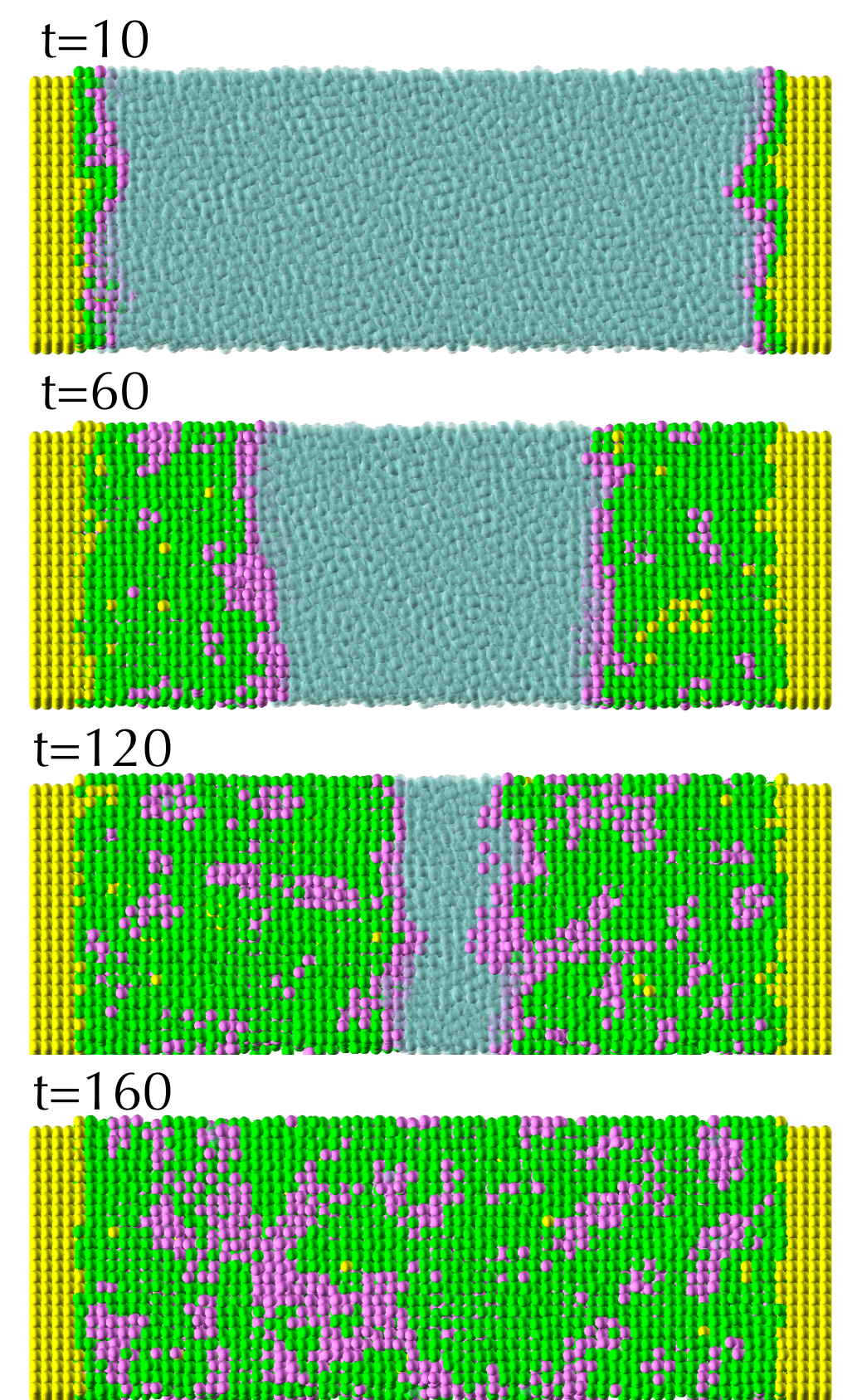


Fig.2. Crystalline growth: perfect, frozen fcc particles (yellow), free fcc particles (green), pre-structured particles (fuchsia) and liquid (turquoise), distinguished using the locally averaged bond order parameters. Pre-structured hcp patches are concentrated at the interfaces.

## 3. Geometrical properties

Averaged local bond order parameters [2] distinguish liquid/solid phases (Fig.2). At the interface (Fig.3) the particles jump from an **hcp** order to the **fcc** stacking.

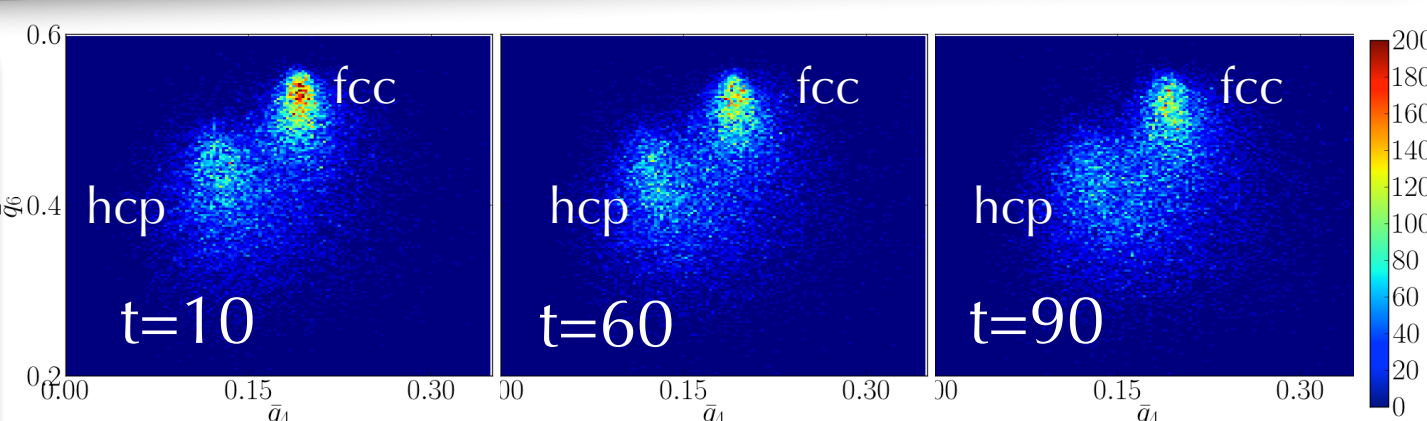


Fig.3. PDF of the averaged local bond order parameters  $\bar{q}_4$  and  $\bar{q}_6$  at different times during the growth (see fig.2 for comparison) for particles in the vicinity of the interface.

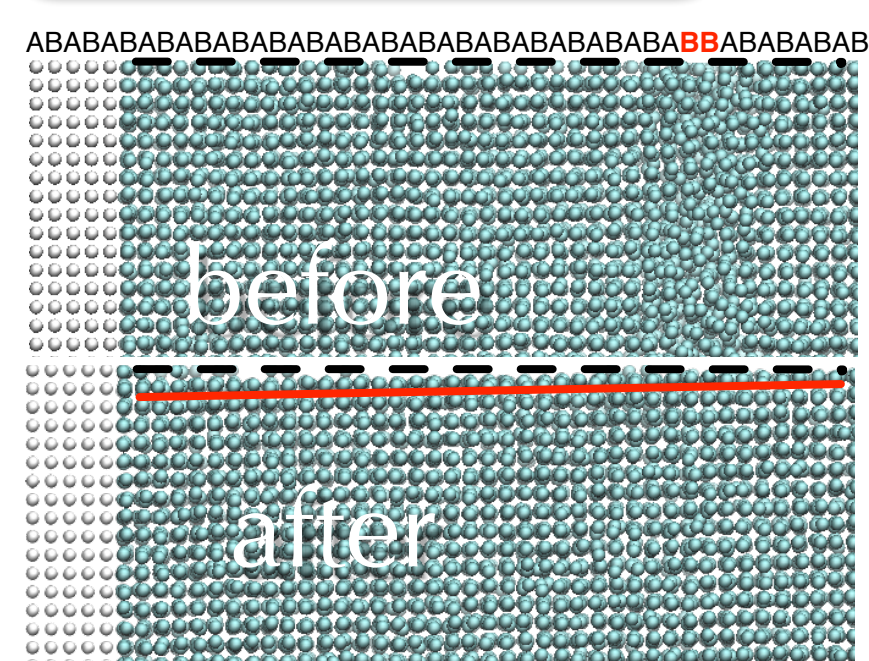


Fig.4. Formation of a dislocation.

After full growth, the ABAB fcc stacking in [100] implies a **defect** when the walls facets are not compatible. The defect is a **dislocation** of all the crystalline planes.

## 4. Modes and interface width

**A few modes** are needed to determine the laterally averaged density profile, correctly matching the position of the interface (fig. 5).

Interface **widths** can be computed from both the density and the  $q_6$  profiles. The scaling  $w \sim t^\alpha$  is different for the two approaches and deviates from the KPZ growth model.

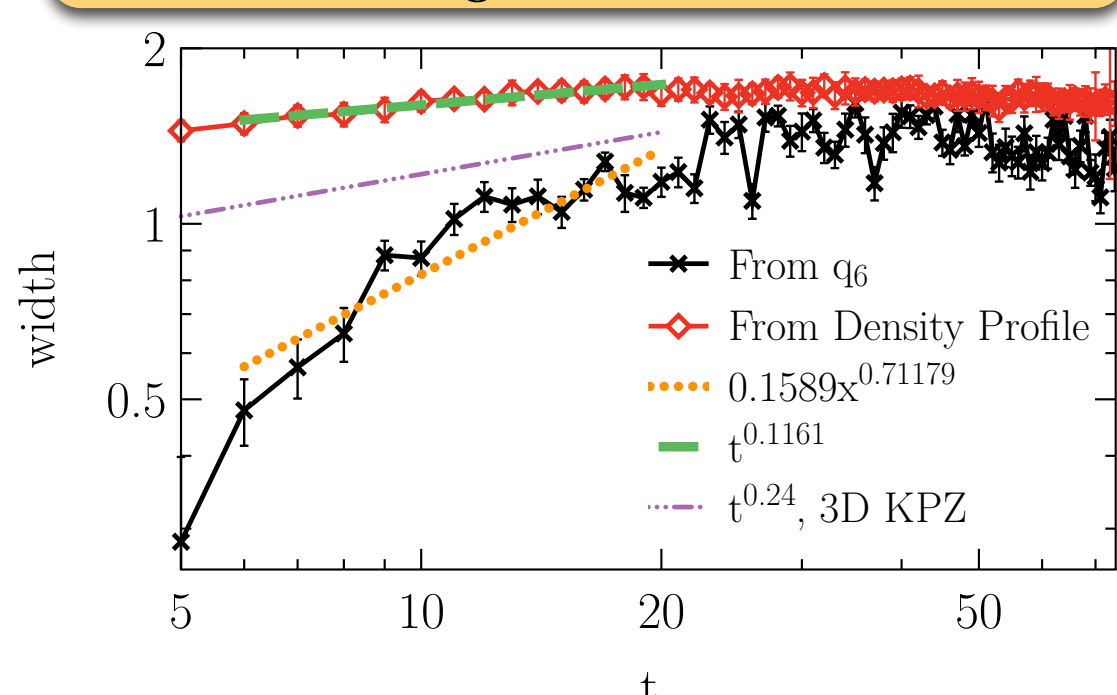


Fig.6. Interface widths computed from the BOP profile and the density profile compared with KPZ predictions.

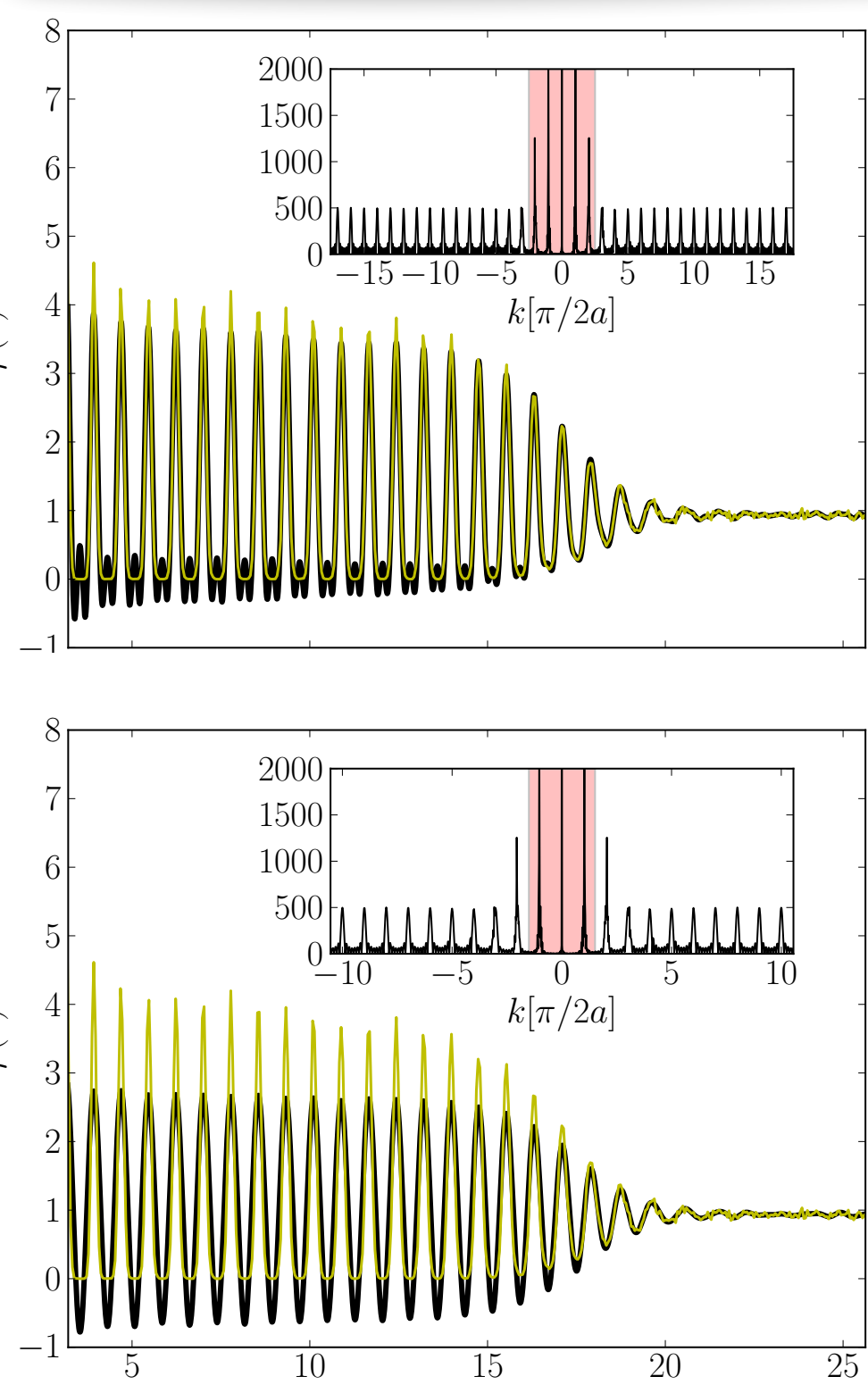


Fig.5. Laterally averaged density profile (yellow) and its reconstruction using low order modes (black) during growth.

## 5. DDFT

Deterministic evolution of the **density field** according to a diffusion-like equation

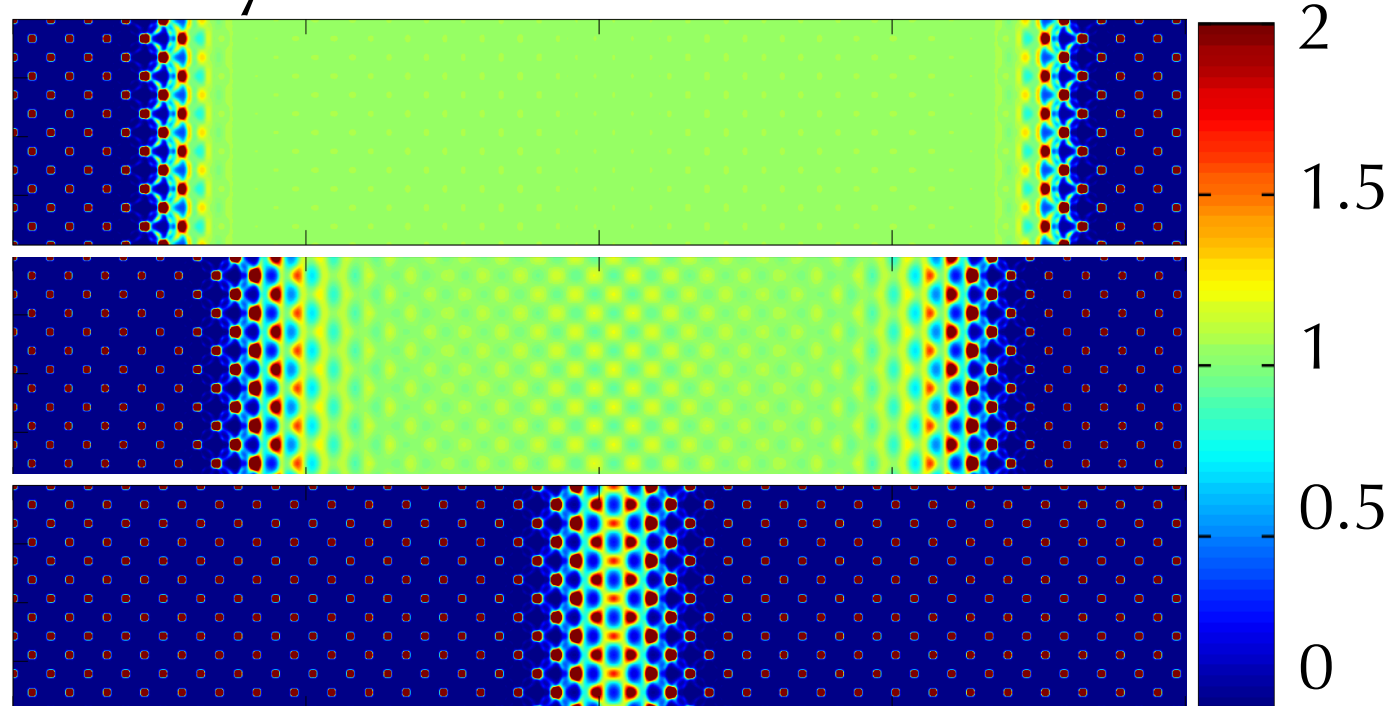
$$\frac{\partial \rho(\vec{r}, t)}{\partial t} = \nabla \left[ \rho(\vec{r}, t) \nabla \left( \frac{\delta F}{\delta \rho} + V^{ext}(\vec{r}) \right) \right]$$

where the chemical potential is chosen according to the **Ramakrishnan-Youssouf** approximation

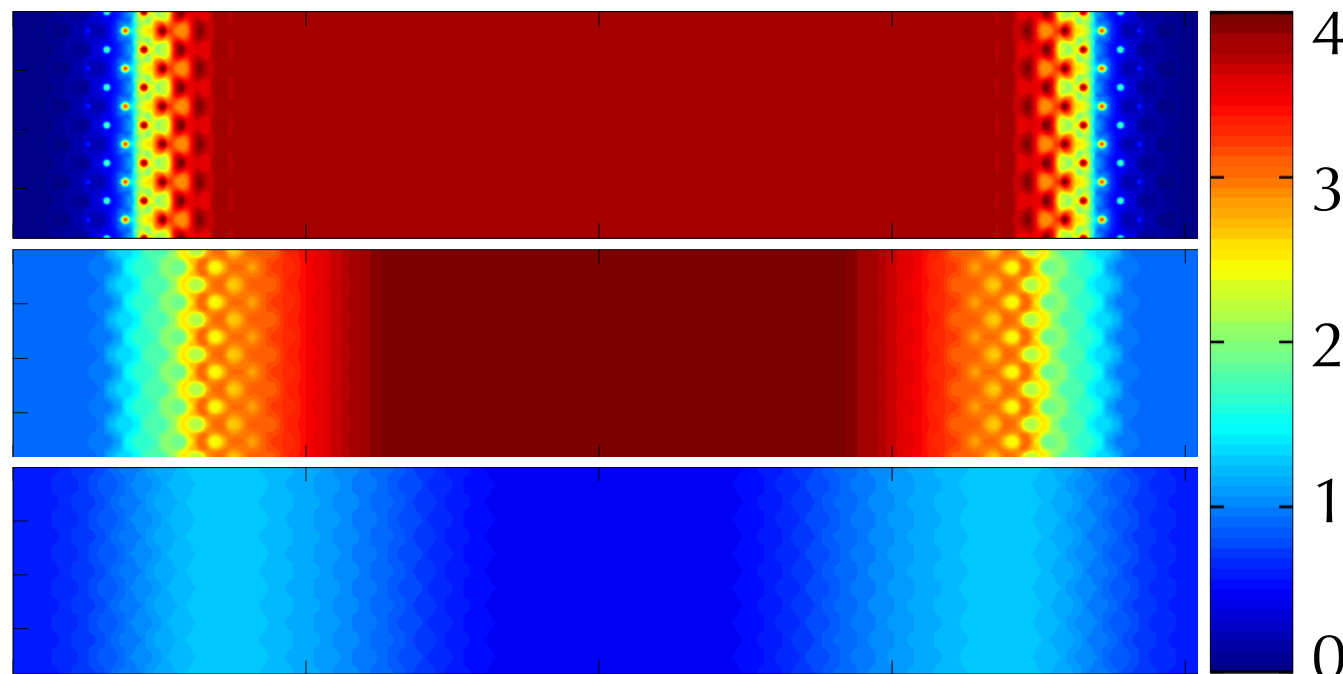
$$\frac{\delta F}{\delta \rho} = \beta^{-1} (\ln \rho - \Delta \rho * c_{ref}^{(2)} + \mu_{ref})$$

with  $c_{ref}^{(2)}$  being the **direct correlation function**, derived via mean field approximation from the pair potential of choice.

**Density field**



**Chemical Potential**



Real-space, discrete-time evolution provides the 3d density field and reproduces the crystal growth.

We have then access to related quantities such as the **free energy**, the **chemical potential** or the **grand potential**.

We will therefore extend previous **equilibrium** work [4] providing a full comparison of the interface properties between the **atomistic** and the **coarse-grained** model.

## References

- [1] H. Emmerich et al. Advances in Physics 61, 665 (2012).
- [2] W. Lechner and C. Dellago, J. Chem. Phys. 129, 114707 (2008).
- [3] E. Marinari et al., J. Phys. A, 33, 8181 (2000).
- [4] M. Oettel et al, Physical Review E 86, 021404 (2012).